

Optically Switching $\chi^{(2)}$ in Diamond Microcavities

Sigurd Flågan,* Joe Itoi, Prasoon K. Shandilya, Vinaya K.

Kavatamane, Matthew Mitchell,† David P. Lake,‡ and Paul E. Barclay

Institute for Quantum Science and Technology, University of Calgary, Calgary, AB, T2N 1N4, Canada

(Dated: December 11, 2024)

Photoinduced modification of second-harmonic generation mediated by nitrogen vacancy (NV) centres in a diamond cavity is observed. Excitation of NV centres quenches the device's second-harmonic emission, and is attributed to modification of $\chi^{(2)}$ by photoionisation from the negative (NV^-) to neutral (NV^0) charge states.

Diamond's excellent optical, thermal, and mechanical properties make it an attractive platform for a myriad of photonics applications [1]. However, its centrosymmetric crystal structure and vanishing $\chi^{(2)} = 0$ limit its use in nonlinear optics to third-order processes, such as four-wave mixing [2] and Raman scattering [3, 4]. Symmetry breaking allows second-order interactions to be observed in centrosymmetric materials. Prominent examples include photogalvanic mediated photoinduced second harmonic generation (SHG) in Si_3N_4 resonators [5, 6] and generation of an effective $\chi_{\text{eff}}^{(2)} = 3\chi^{(3)}E_{\text{DC}}$ in silicon by a charged-defect induced DC electric field, E_{DC} [7]. In diamond, SHG has recently been observed using ultrafast laser pulses interacting with a $\chi^{(2)} \neq 0$ region formed through symmetry breaking from a shallow (35 nm deep) high density ($3 \times 10^{17} \text{ cm}^{-3}$) layer of nitrogen vacancy (NV) centre defects [8, 9].

In this work, we control the strength of diamond SHG using an optical field that excites NVs in the material. Using a nanophotonic diamond cavity we generate SHG from a continuous telecommunication wavelength field and observe, for the first time, that diamond's effective $\chi^{(2)}$ changes when the charge state of NVs hosted by the crystal is modified. This effect allows optical control of diamond's optical nonlinearity and provides insight into the influence of NVs on $\chi^{(2)}$.

The device used here is a microdisk (Fig. 1 (a)) fabricated from a single crystal optical grade diamond chip hosting a uniform distribution of NV centres (density $\sim 10^{13} - 10^{14} \text{ cm}^{-3}$ [10]). The microdisk supports optical whispering gallery modes with quality factors $Q = 10^3 - 10^5$ [11] that are evanescently coupled to a fibre taper waveguide. It is positioned in the focus of a confocal microscope that excites NV centre photoluminescence (PL) with a green (532 nm) laser [11]. Second harmonic generation is excited using a tunable laser ($P_{\text{IR}} = 76 \text{ mW}$) coupled to a microdisk mode (wavelength $\lambda_{\text{IR}} \sim 1547 \text{ nm}$) via the fibre taper, whose transmission spectrum is shown in Fig. 1 (b). Second harmonic generation is further enhanced by a cavity mode at $\lambda_{\text{IR}}/2$ and

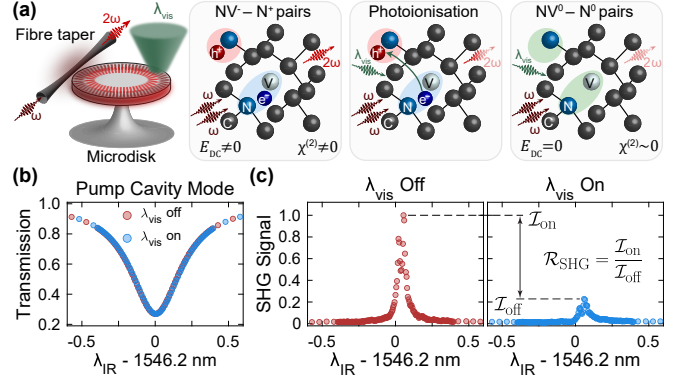


FIG. 1. (a) A schematic of the fibre coupled diamond microdisk system used to demonstrate optically modulated SHG, and a proposed mechanism for the observed behaviour of $\chi^{(2)}$. An electric field (E_{DC}) created by negatively charged NV centres induces an effective $\chi_{\text{eff}}^{(2)} \neq 0$. Photoionisation by a green wavelength (λ_{vis}) field combined with the IR field modifies χ_{eff} , quenching SHG. (b) Normalised fibre-taper transmission spectrum of the pump mode, showing that it is unaffected by the green illumination. (c) SHG signal in the absence (burgundy) and presence (blue) of green illumination. Data in blue has been corrected for background PL from NV centres.

is collected by the same fibre taper. The impact of the device's double resonance is shown in Figure 1 (c): SHG is only observed with the IR field on resonance, and is strongest for a slight red detuning where $\lambda_{\text{IR}}/2$ is also resonant with a mode.

To probe the effect of NV centres on $\chi^{(2)}$, we optically excite them with the green laser focused on the microdisk edge while monitoring SHG. We observe strong quenching of the SHG intensity by the green laser (Fig. 1 (c)). To rule out laser-induced modification of the microdisk mode wavelengths, we monitor the pump mode (Fig. 1 (b)) and a cavity enhanced third-harmonic signal (not shown), and observe no change to either.

The quenching of SHG under green excitation points to defects such as NV centres being key contributors to $\chi^{(2)}$, as observed with charge traps in silicon [7]. We write the second-order nonlinear susceptibility as $\chi_{\text{eff}}^{(2)} = \chi_{\text{host}}^{(2)} + \chi_{\text{NV}}^{(2)}$ [12], where $\chi_{\text{NV}}^{(2)}$ can be affected by modification of the NV electronic state, while $\chi_{\text{host}}^{(2)}$ may be attributed to other properties of the device. Two

* sigurd.flagan@ucalgary.ca

† Currently with Dream Photonics Inc., Vancouver, BC, V6T 1Z4, Canada

‡ Currently with the Applied Physics Department, California Institute of Technology, Pasadena, CA 91125, USA

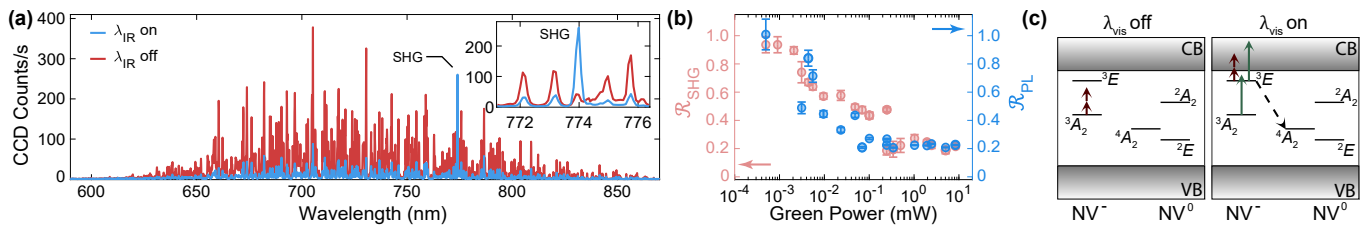


FIG. 2. **(a)** Fibre taper collected NV PL spectrum generated by green illumination of the microdisk. Coupling a strong IR field into the microdisk suppresses the PL. **(b)** The correlation between SHG quenching and PL suppression, shown by the strength of SHG (pink, left) and NV centre PL (blue, right) for varying green laser power. **(c)** Relevant energy levels of NV^0 and NV^- . Burgundy and green arrows represent IR (λ_{IR}) and green photons (λ_{vis}), respectively. (*left*) Under λ_{IR} excitation, higher-order photon (> 2) processes are required to excite NV^- and population remains in NV^- . (*right*) Green photons promote population from NV^- 's 3A_2 ground to its 3E excited state, where two IR photons can pump the NV into the dark 4A_2 state of NV^0 (black dashed arrow).

NV related optical processes could lead to quenching. First, green excitation cycles the predominantly negatively charged NV^- defects between their 3A_2 ground state and the 3E excited state [13], generating PL as shown by the spectra in Fig. 2(a). The average change in electron configuration during this cycling may change $\chi_{NV}^{(2)}$; in this case the SHG quenching would imply a smaller $\chi_{NV}^{(2)}$ for the 3E state than for the 3A_2 state. Second, the combination of green and IR fields can modify the NV charge state by photoionising NV^- to a dark state of NV^0 [14]. This process is illustrated Fig. 2(b), and revealed experimentally in Fig. 2(a) by the IR field's suppression of NV centre PL collected by the fibre taper. It requires excitation by a green photon to the 3E state of NV^- followed by photoionisation to the 4A_2 state of NV^0 via a single green photon or two IR photons. For high IR intensity created within the high- Q microdisk the nonlinear process dominates and traps population in the dark 4A_2 state [14]. This explanation implies that NV^0 possesses a smaller $\chi_{NV}^{(2)}$ than NV^- or that the change in local charge environment when NV^- is converted to NV^0 affects $\chi_{eff}^{(2)}$.

To test these explanations, we measure the SHG quenching for varying green excitation power, as shown in Fig. 2(b). Here we define relative SHG intensity as $\mathcal{R}_{SHG} = \mathcal{I}_{on}/\mathcal{I}_{off}$, where $\mathcal{I}_{on(off)}$ is the SHG peak intensity in the presence (absence) of green excitation. For comparison, we also plot the corresponding suppression of PL, defined as $\mathcal{R}_{PL} = \mathcal{L}_{on}/\mathcal{L}_{off}$ where $\mathcal{L}_{on(off)}$ is PL integrated over the NV^- emission band of 640 nm to 770 nm in the presence (absence) of the IR field. The strong correlation between the quenching of the SHG and suppression of the PL points toward a similar underlying mechanism, namely IR assisted photoionisation to NV^0 [14]. Note that when measuring \mathcal{R}_{SHG} we account for PL emitted into the SHG mode by first measuring it

in absence of the IR field, and then assuming that it is suppressed by the IR field in equal proportion as the PL into other nearby modes (inset Fig. 2(a)).

As introduced above, the $\chi^{(2)}$'s dependence on NV charge state can arise for several mechanisms. Most directly, the microscopic $\chi_{NV}^{(2)}$ determined by the electronic structure of NV^0 may be smaller than that of NV^- ; this is consistent with *ab initio* calculations [12]. In addition, the local charge environment and electric field created by the NV^- ensemble could induce a $\chi_{host}^{(2)}$ that is quenched when it is converted to NV^0 . For example, the ionisation process $NV^- + N^+ \rightarrow NV^0 + N^0$ reduces the local charge environment by two [15]. This effect, illustrated in Fig. 1(a), has been studied in SHG in silicon devices induced by charges from impurities [7] and depletion layers [16], and may be affected by the density of other impurities such as nitrogen, as well as device geometry and its effect on electron accumulation. Further measurements, particularly in the time domain, are required to definitively identify the dominant mechanism.

In conclusion, we have demonstrated optical modification of SHG from a diamond microdisk cavity mediated by NV centres, and have shown the device's $\chi^{(2)}$ strongly depends on NV charge-state. A deeper understanding of the relationship between $\chi^{(2)}$ and the charge-state provides the foundation for frequency conversion and optical switching via $\chi^{(2)}$ engineering – a valuable addition to the diamond photonics arsenal.

ACKNOWLEDGMENTS

This work was supported by NSERC (Discovery Grant program), Alberta Innovates, and the Canadian Foundation for Innovation. SF acknowledges support from the Swiss National Science Foundation (Project No. P500PT.206919).

[1] P. K. Shandilya, S. Flagan, N. C. Carvalho, E. Zohari, V. K. Kavatamane, J. E. Losby, and P. E. Barclay, Dia-

mond Integrated Quantum Nanophotonics: Spins, Pho-

- tons and Phonons, *Journal of Lightwave Technology* **40**, 7538 (2022).
- [2] B. J. M. Hausmann, I. Bulu, V. Venkataraman, P. Deotare, and M. Lončar, Diamond nonlinear photonics, *Nature Photonics* **8**, 369 (2014).
- [3] D. Riedel, S. Flågan, P. Maletinsky, and R. J. Warburton, Cavity-Enhanced Raman Scattering for In Situ Alignment and Characterization of Solid-State Microcavities, *Physical Review Applied* **13**, 014036 (2020).
- [4] S. Flågan, P. Maletinsky, R. J. Warburton, and D. Riedel, Microcavity platform for widely tunable optical double resonance, *Optica* **9**, 1197 (2022).
- [5] X. Lu, G. Moille, A. Rao, D. A. Westly, and K. Srinivasan, Efficient photoinduced second-harmonic generation in silicon nitride photonics, *Nature Photonics* **15**, 131 (2021).
- [6] E. Nitiss, J. Hu, A. Stroganov, and C.-S. Brès, Optically reconfigurable quasi-phase-matching in silicon nitride microresonators, *Nature Photonics* **16**, 134 (2022).
- [7] C. Castellan, A. Trenti, C. Vecchi, A. Marchesini, M. Mancinelli, M. Ghulinyan, G. Pucker, and L. Pavesi, On the origin of second harmonic generation in silicon waveguides with silicon nitride cladding, *Scientific Reports* **9**, 1088 (2019).
- [8] A. Abulikemu, Y. Kainuma, T. An, and M. Hase, Second-Harmonic Generation in Bulk Diamond Based on Inversion Symmetry Breaking by Color Centers, *ACS Photonics* **8**, 988 (2021).
- [9] A. Abulikemu, Y. Kainuma, T. An, and M. Hase, Temperature-dependent second-harmonic generation from color centers in diamond, *Optics Letters* **47**, 1693 (2022).
- [10] V. M. Acosta, E. Bauch, M. P. Ledbetter, C. Santori, K.-M. C. Fu, P. E. Barclay, R. G. Beausoleil, H. Linget, J. F. Roch, F. Treussart, S. Chemerisov, W. Gawlik, and D. Budker, Diamonds with a high density of nitrogen-vacancy centers for magnetometry applications, *Physical Review B* **80**, 115202 (2009).
- [11] T. Masuda, J. P. E. Hadden, D. P. Lake, M. Mitchell, S. Flågan, and P. E. Barclay, Fiber-taper collected emission from NV centers in high-Q/V diamond microdisks, *Optics Express* **32**, 8172 (2024).
- [12] P. Li, X. Jiang, M. Huang, L. Kang, S. Chen, A. Gali, and B. Huang, Defect engineering of second-harmonic generation in nonlinear optical semiconductors, *Cell Reports Physical Science* **3**, 101111 (2022).
- [13] A. Gali, M. Fyta, and E. Kaxiras, Ab initio supercell calculations on nitrogen-vacancy center in diamond: Electronic structure and hyperfine tensors, *Physical Review B* **77**, 155206 (2008).
- [14] P. K. Shandilya, V. K. Kavatamane, S. Flågan, D. P. Lake, D. Sukachev, and P. E. Barclay, Nonlinear optical pumping to a diamond NV center dark state, arXiv: 2411.10638 (2024).
- [15] N. B. Manson, M. Hedges, M. S. J. Barson, R. Ahlefeldt, M. W. Doherty, H. Abe, T. Ohshima, and M. J. Sellars, $NV^- - N^+$ pair centre in 1b diamond, *New Journal of Physics* **20**, 113037 (2018).
- [16] E. Timurdogan, C. V. Poulton, M. J. Byrd, and M. R. Watts, Electric field-induced second-order nonlinear optical effects in silicon waveguides, *Nature Photonics* **11**, 200 (2017).